# Decoding Future Tropical Cyclone Impact: Unveiling the Roles of Urbanization and Climate Change

Sven Bastiaan Kooistra

September 2023 - March 2024

Student number: 6252435
E-mail: s.b.kooistra@students.uu.nl
First supervisor: Jaap Nienhuis
Second supervisor: Wilco Hazeleger
MSc Programme: Earth Surface and Water
Faculty of Geosciences
Department of Physical Geography
Utrecht University, the Netherlands

## Abstract

Studies suggest that damages from extreme weather events, such as tropical cyclones (TCs), are on the rise even without the direct effects of climate change (CC), with urbanization due to socioeconomic development as the main driver. The rise in material assets vulnerable to tropical storms constitutes a significant factor contributing to potential future losses. CC could intensify TCs on top of that. Increased rainfall and rising sea levels are among the main drivers of the increase in future impact. However, the composition of future TC impacts is still underexplored. This study showed that urban growth contributes to future TC impact. Urbanization was, for every possible SSP/RCP scenario, responsible for more than 50% of the modeled impact. More extreme RCP scenarios impact attributable to CC increased significantly from 6.1% to 45.2% across the RCP scenarios. The results of this study show that policymakers should focus on controlled urbanization using spatial planning and building codes. These results emphasize integrating socioeconomic variables, such as urban, into future TC risk assessments. This study served as a foundation for more sophisticated future TC impact assessments. For example, future TC risk assessments should include compound events, such as TC surges and flooding due to rainfall. Lastly, future studies should perform a more profound analysis of the relationship between urban land use and exposure to improve the robustness of future TC impact assessments.

# Contents

# 1 Introduction

Tropical Cyclones (TC) are formidable natural phenomena (Collins and Walsh, 2017). TCs caused around $945.9 billion in damages from 1980 to 2019 (Smith, 2020), which is, according to the NOAA's National Centers for Environmental Information, more than half of the total damages caused by weather and climate disasters (Smith, 2020). Empirical evidence suggests that tropical cyclone impacts can hinder economic growth in affected countries for over a decade (Krichene et al., 2023). Moreover, the NOAA states that TCs are responsible for 6,502 of the 13,246 deaths caused by weather and climate events (Smith, 2020). Most damages during tropical storms are water-related, such as surges and rainfall. The most frequent hazard occurring is rainfall-induced flooding (Kim et al., 2022).

Studies suggest that damages from extreme weather events, such as TCs, are on the rise due to urbanization as a result of socioeconomic development playing a significant role (Freeman and Ashley, 2017). The Intergovernmental Panel on Climate Change (IPCC) asserts that the rise in material assets vulnerable to tropical storms constitutes a significant factor contributing to potential future losses (Schmidt et al., 2009). A comprehensive breakdown of these impacts, especially regarding future proportions between climate change-related and urbanization-related impacts, remains challenging (Meiler et al., 2023).

Climate change (CC) could intensify TCs on top of that (Wu et al., 2022), though some argue more evidence is needed (Mendelsohn et al., 2012). CC may increase the volume of rainfall linked to tropical storms and TCs (Smiley et al., 2022). Some predictions estimate an increase 35% in rainfall due to CC (Liang and Liu, 2020). Sea level rise (SLR) can also increase storm damage (Yin, 2023). SLR influences the height of the storm surges, which are huge waterbodies propelled by the powerful wind fields of TCs.

Probabilistic natural catastrophe risk models serve as a quantitative foundation for analyzing risk and developing mitigation strategies (Eberenz et al., 2021). There has been a growing need for global-scale TC risk assessments since the mid-2000s (Ward et al., 2020). Previous studies evaluated economic risk utilizing historical TC data (Cardona et al., 2014). Researchers currently use simulations based on tropical cyclone records generated by downscaling global climate models to project future tropical cyclone risk (Korty et al., 2017). TC Risk models depend on hazard, exposure, and the vulnerability of the affected region (Eberenz et al., 2021). Physical characteristics of a TC, such as wind speed, are all part of the hazard component (Aznar-Siguan and Bresch, 2019). The number of people or the amount of assets in a region determines exposure (Geiger et al., 2018).

The devastating impact of TCs in the United States exemplifies the extensive challenges created by TCs in developed and highly urbanized regions (Senkbeil et al., 2011). This study uses a previous TC and simulates the impact in future scenarios. TC Irma, which terrorized the South of Florida, is used. Irma's catastrophic nature and widespread damage emphasize the importance of understanding the complex interplay between TC impact, socioeconomic development, and CC (Mitsova et al., 2018). The frequency and intensity of TCs like Irma will likely increase in the future (Done et al., 2018). The amount of change depends on of these properties depends on the climate scenario, which is established within Representative Concentration Pathways (RCPs) (Jewson, 2021). The geographical location of Florida, along with its developed socioeconomic status, makes it an excellent case study for this research. Florida's coastal communities and cities are particularly susceptible to TCs (Coughlin et al., 2009).

This research addresses the underexplored composition of future TC impacts, dissecting the roles of urbanization and CC and focusing on their economic ramifications. The study seeks to understand the cumulative effects of these factors on societies susceptible to TCs. By better understanding the composition of TC impact, governments and stakeholders can design more accurate mitigation strategies (Ye et al., 2020).

The primary objective is to explore the amount of impact attributed to induced socioeconomic development-induced urbanization and more extreme tropical cyclones due to CC in future scenarios. By integrating urban land cover change projections into a climate model, this study seeks to correlate exposure with urban land cover change, comprehensively assessing the composition of future TC impacts. Urban land use is chosen as an indicator of socioeconomic development because that is where, during extreme climate events, the interplay between infrastructural, environmental, and socioeconomic systems is exposed (Simpson et al., 2021). The main research question is: “What is the composition impact of future tropical cyclones impact, and what are the respective contributions of socioeconomic development and climate change?”

This study uses a multifaceted research approach that combines data analysis, modeling techniques, and case study analysis to investigate the composition of TC impact. Data sources include a CLImate ADAptation tool (CLIMADA) and future urban land cover projections based on SSPs. These sources will facilitate the assessment of exposure, socioeconomic development, and urban land cover change.

## 2 Methods

The workflow consisted of multiple steps (Fig. 1). Firstly, a climate adaption model (CLIMADA) was used to assess current exposure. Additionally, CLIMADA was used to perform impact calculations for a “base year” situation. CLIMADA is a tool that uses a probabilistic natural hazard model to assess the potential impact presented by future TCs and lays out a robust framework for impact assessments (Aznar-Siguan and Bresch, 2019).

Secondly, integrated assessment models, SSPs, presented future socioeconomic development through urban land expansion.(O'Neill et al., 2017). This study used the SSP2 scenario and SSP5 scenarios. A global 1-km downscaled Urban Land extent projection by SSP scenarios was used to assess urban land cover change based on socioeconomic development because the urban landscape is an essential indicator of socioeconomic dynamics (Gao and Pesaresi, 2021). With this socioeconomic indicator and the exposure data from CLIMADA, it was possible to examine whether there was a potential relationship between these two factors and whether this relationship was suitable for analyses for future exposure projections.

Thirdly, a case study of TC Irma, alongside constructed exposure projections, was utilized to evaluate the proportions of impact attributed to urbanization and CC on projected TC impact for current and future assessments. This case study included the evaluation of proportions caused by urban growth and CC. Conducting a current impact assessment of Irma and subsequently situating the same hurricane within various future climate and socioeconomic scenarios garnered valuable insights into the evolution of TC impact and its composition in the future. This approach contributed to a clearer understanding of the intricate relationship between TC impact, urbanization, and CC. CLIMADA utilized the already implemented exposure dataset and calculated the impact of TC Irma. This dataset was then employed to assess the intricate relationship between exposure and urban land cover, subsequently informing the computation of future TC exposure using the SSP-based urban land use datasets. Furthermore, this study used these projected tropical cyclone exposure maps to conduct future impact assessments. Initially, they only included urban land cover change, and subsequently, they incorporated both urban land cover change and the growing impact of tropical cyclones due to CC.

Lastly, this research assessed the CLIMADA model's strengths and limitations in capturing the impacts of land-use change on TC exposure. We also evaluated its reliability and applicability in different geographical and climatic contexts relevant to this study.

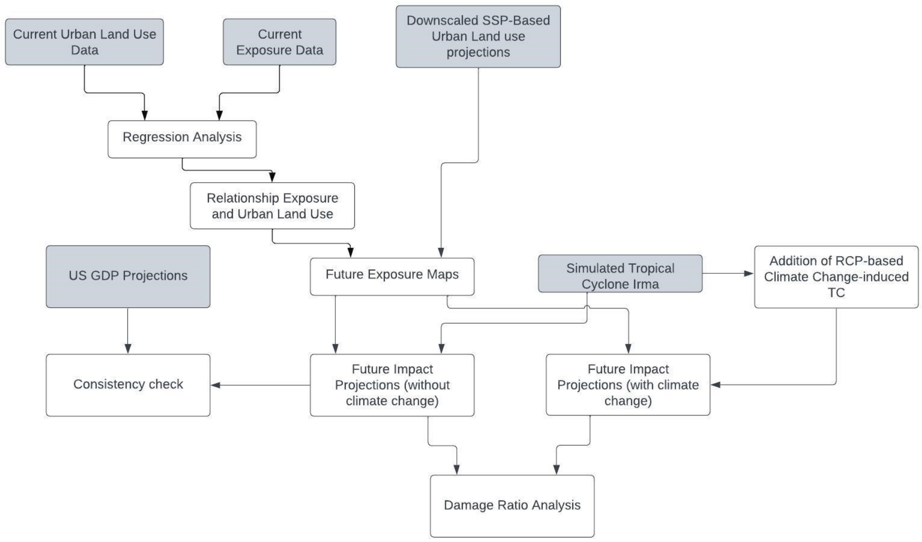


Figure 1: Flowchart of the workflow of this study

## 2.1 Data Collection

### 2.1.1 Exposure Data

CLIMADA contains gridded asset exposure data Eberenz et al. (2020). Eberenz et al. (2020) propose a methodology for generating a high-resolution asset exposure map that involves breaking down the overall asset value of each country. Dissecting this country-level asset value was performed using nightlight luminosity and population data. These two variables were separately integrated through linear interpolation to 30-arcsecond resolution gridded datasets. Subsequently, the two datasets were combined for every grid cell using Equation 1:

$$(\mathrm{Lit})^n \cdot \left(\mathrm{Pop_{pix}}\right)^m = (\mathrm{NL_{pix}} + \delta)^n \cdot \left(\mathrm{Pop_{pix}}\right)^m \tag{1}$$

Where $\mathrm{NL_{pix}}$ is the nightlight intensity of a grid cell and has a value between 0 to 255 because that is the derived scale for nightlight intensity, $\mathrm{Pop_{pix}}$ represents the population count and is made up of a real positive number. The exponents $n$ and $m$ are integers, where $m > 0$, $\delta$ is set to 1 to prevent non-illuminated but populated grid cells from being lost. Exponent $m$ is set to zero for grid cells without population data.

Following this step, Eberenz et al. (2020) used the gathered $\mathrm{Lit}^n\mathrm{Pop}^m$ to disaggregate country-level asset values linearly. Hence, it creates a representation of economic stocks per geographical grid cell. In other words, every grid cell represents a value of $\mathrm{Lit}^n\mathrm{Pop}^m$ relative to the sum of the $\mathrm{Lit}^n\mathrm{Pop}^m$ values of all pixels, as illustrated in the following Equation:

$$I_{\mathrm{pix}} = I_{\mathrm{tot}} \frac{\mathrm{Lit}^n \cdot \mathrm{Pop}^m_{\mathrm{pix}}}{\sum^N_{\mathrm{pix}_i} (\mathrm{Lit}^n \cdot \mathrm{Pop}^m_{\mathrm{pix}_i})} \tag{2}$$

Here, $I_{\mathrm{pix}}$ represents the asset value per grid cell. The country-level asset value is $I_{\mathrm{tot}}$ and is distributed relative to every grid cell's $Lit^m Pop^m$ share. $N$ is the total number of grid cells within the relevant country. Exponents $m$ and $n$ are relative between $Lit$ and $Pop$ and crucial in determining the difference in the distribution of the total amount of grid cells. Changing $m$ and $n$ dictates with which power *Lit* and *Pop* contribute to the disaggregation function. Figure 2 represents the workflow explained above.

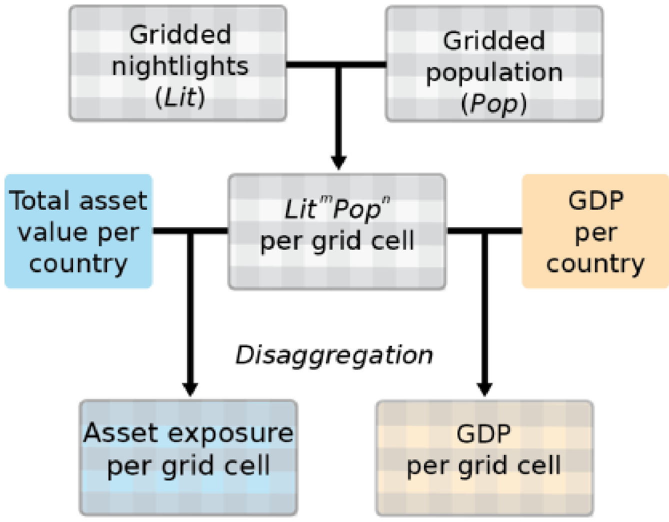


Figure 2: Workflow of the LitPop class in CLIMADA (Eberenz et al., 2020)

Higher asset concentrations meant higher degrees of exposure (Fig. 3). These areas of higher exposure showed a correlation between urban land use and exposure. Cities with large urban cores, such as Tampa and Orlando, showed well-defined pattern impact compared to more rural areas. This relationship highlighted the critical role of urban growth in influencing TC exposure.

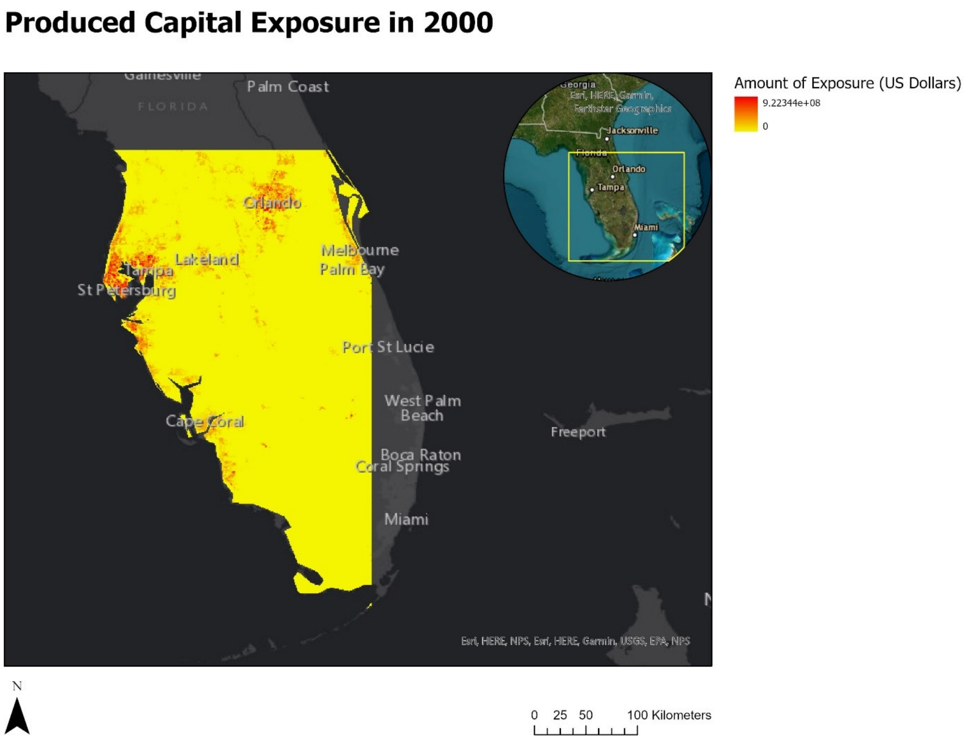


Figure 3: PC exposure of South Florida in 2000.

### 2.1.2 Urban Land Use Data

Implementing urban land use data made analyzing the intricate dynamics between socioeconomic development, CC, and tropical cyclone impact possible. Urban land use is one of the characteristics of socioeconomic development (Li et al., 2014). By using downscaled urban land use projections, translating those into exposure projections, and integrating them into CLIMADA, an accurate method was developed for quantifying future tropical cyclone impact due to urban land use change. This study's urban land use data was a downscaled Urban Land Extent Projection based on different Shared Socioeconomic Pathway (SSP) scenarios (Gao and Pesaresi, 2021). The data was available from the Socioeconomic Data and Applications Center (SEDAC). Each SSP scenario contains projections for the urban land use for several years up until 2100. Gao and Pesaresi (2021) obtained these urban land use projections by downscaling the original 1/8th degree urban expansion maps developed by Gao and O'Neill (2020), consistent with the SSP scenarios. This section will briefly explain the original downscaling process by Gao and O'Neill (2020), followed by the second downscaling procedure by Gao and Pesaresi (2021).

**Downscaling to 1/8th degree grid cells**

Goa & O'Neill (2020) propose a downscaling method that uses a combination of two urban simulation models (Fig. 4): The Spatially, Long-term, Empirical City developmenT (SELECT) and The Country-Level Urban Buildup Scenario (CLUBS). CLUBS projects the total new amount of urban land, and SELECT was used to allocate the new urban land based on the country's potential for development.

CLUBS creates scenarios to project the amount of country-specific new urban land developed every

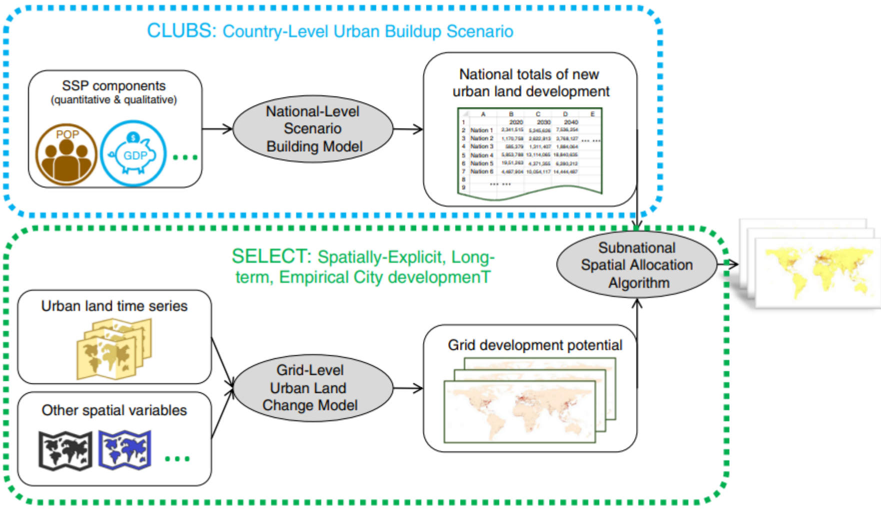


Figure 4: Framework of the downscaling procedure as proposed by Goa & O'Neill (2020).

decade of the 21st century. These projections depend on GDP, population size, and other SSP-based socioeconomic trends. Goa & O'Neill used historical economic growth and urbanization data to create the model. The model combines quantitative Monte Carlo experiments and qualitative analysis of SSP narratives to predict the amount of urban growth accurately. CLUBS establishes the likelihood of a particular urban growth rate for region-specific urbanization style. The Monte Carlo Experiments generate 1000 model urban expansion rate alternatives. A high, medium, or low estimate is chosen based on a country's urbanization style and SSP scenario.

SELECT allocates the new urban land predicted by the CLUBS model in 1/8th-degree grid cells. Urban land development potential is determined based on historical data. Changes in urban land were derived from remote sensing imagery and global data on environmental factors and population dynamics. The world is divided into 375 subnational regions, where each region is based on existing cities and modeled individually using a Generalized Additive Model (GAM). The advantage of using a GAM is that it can adapt to regional dynamics and recognize relevant parameters that drive urban land change. This way, both local variations and global urban growth dynamics are used.

**Downscaling to 1km grid cells**

The downscaling of the projections, as proposed by Goa & Pesaresi (2021), was done by using a spatial scalar (Equation 3), updated at the start of each decade to assign urban land expansion to 1-km grid cells proportionally.

$$\text{Spatial Scalar}_{1km} = \frac{\text{Total Urban Land}_{1km}}{\text{Total Urban Land}_{(1/8\text{degree})}} \tag{3}$$

Equation 3 shows that the spatial scalar is determined by the amount of urban land present in a 1/8-degree grid cell. More existing land leads to a higher allocation of new urban land expansion. The downscaling algorithm used a proportional allocation method for urban growth; however, in some cases, it may surpass available land in particular 1 km grid cells.

Excess allocations within a 1/8-degree grid cell were redistributed among 1 km grid cells with available land until no overflow occurred. This procedure was repeated every step until there was no overflow. The algorithm first filled up somewhat developed cells in cases where the 1/8-degree grid cell had more urban land expansion than the total available land from grid cells, which had been developed to some degree (Equation 4).

$$\text{Spatial Scalar}_{1km}^{\text{supplementary}} = \frac{\text{Total Available Land}_{1km}}{\text{Total Available Land}_{(1/8\text{degree})}} \tag{4}$$

Figure 5 displays the theoretical workflow of the downscaling algorithm to 1km grids.

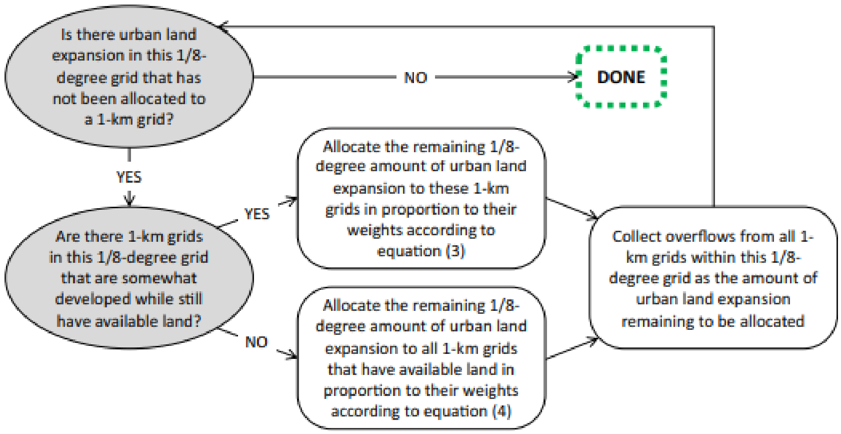


Figure 5: theoretic workflow of the downscaling algorithm of the urban land use data to 1km grid cells (Gao and Pesaresi, 2021)

The spatial distribution in Florida varies from a high fraction of urban land in the downtown areas of cities such as Tampa and Orlando to a low fraction of urban land use in the rural areas (Fig. 6).

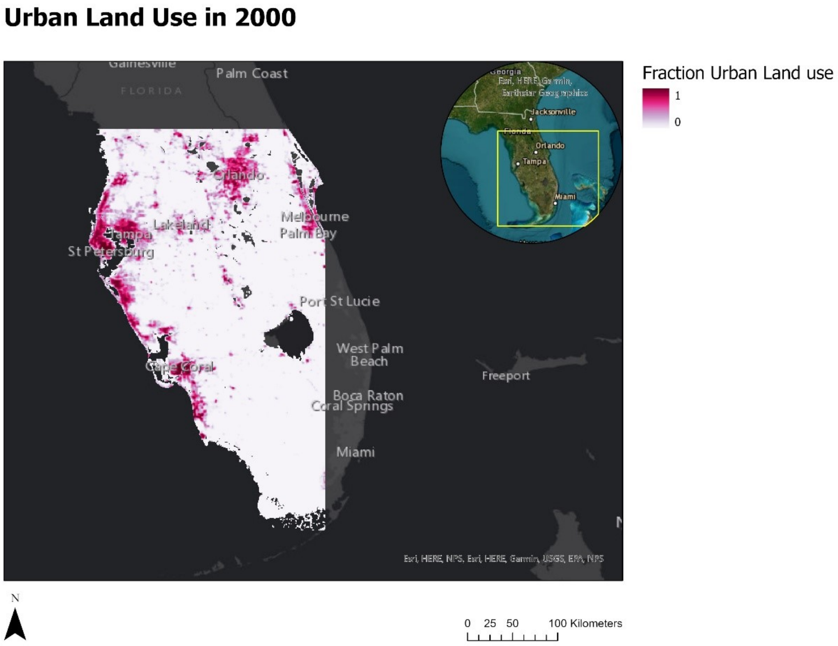


Figure 6: Urban Land use in 2000 (Gao and Pesaresi, 2021)

## 2.2 Impact Assessment for Current Situation

### 2.2.1 Selection of Exposure Indicators

This study used Produced Capital (PC) to assess TC exposure. PC in World Bank wealth accounts includes manufactured assets and values urban land by applying a markup to other produced assets (Wodon and Carey, 2018), which is why it was most appropriate for correlating with urban land use

### 2.2.2 CLIMADA Model Configuration

The calculation of damage involved applying the impact function from Emanuel et al. (2011) to model TC impact. This model facilitated the computation of TC properties based on imported TCs (Aznar-Siguan and Bresch, 2019). Historic TC tracks from the International Best Track Archive for Climate Stewardship (IBTrACS) archive were available within CLIMADA (Aznar-Siguan and Bresch, 2019).

The information about the eye included in a tropical cyclone track was the location, time, central and environmental properties, and radius of maximum wind speeds (Aznar-Siguan and Bresch, 2019). Subsequently, 1-minute sustained peak gusts were calculated by combining a static circular wind field with the translational wind speed generated by the storm's movement (Aznar-Siguan and Bresch, 2019). The reduction in the translational component from the cyclone center was factored in through multiplication by an attenuation factor (Aznar-Siguan and Bresch, 2019).

The impact function from Emanuel (2011) states that property damage only occurs if wind speeds exceed a certain threshold value, determined at 25.7 m $s^{-1}$. Property damage increases cubically with the wind speed (Equation 5 & 6) (Aznar-Siguan and Bresch, 2019):

$$f_{ij} = \frac{v_{ij}^3}{1 + v_{ij}^3} \tag{5}$$

$$v_{ij} = \frac{\max(v_{ij} - v_{\text{thresh}}, 0)}{v_{\text{half}} - v_{\text{thresh}}} \quad (6)$$

Where $v_{\text{half}} = 74.7$ m s$^{-1}$ and represents the wind gusts when half of the property is damaged (Aznar-Siguan and Bresch, 2019). Moreover, $v_{ij}$ represents the maximum wind gust at centroid $i$ and caused by event $j$ (Aznar-Siguan and Bresch, 2019).

### 2.2.3 Execution of Impact Assessment

With an impact assessment of the "current climate," it was possible to establish a base for future impact assessments. It was possible to see the spatial distribution of the modeled damages and how hazard and exposure translated to impact. The spatial distribution of the modeled impact was important because future impact patterns should be similar to the current and hence could serve as a consistency check.

During the impact analysis, this research simulated TC Irma's track on the high-resolution exposure map from the base year. The outcome was a value representing the total modeled impact on the research area. Additionally, CLIMADA computed an impact data frame of the research area, illustrating where the most significant impact was likely to occur.

## 2.3 Regression Analysis

This section outlines the regression analysis used to explore the relationship between exposure and urban land use. This relationship was the driving factor in constructing future exposure maps. Firstly, it was made sure that both datasets had identical spatial dimensions and resolution. This study performed the regression analysis between exposure and urban land use for the determined "base year" situation, set as 2000 in the urban land use data. The regression analysis was done using several regression models. The model with the highest resulting R-squared value was selected for constructing future exposure maps, which was widely used as a goodness-of-fit measure (Cameron and Windmeijer, 1997). The selected regression model was executed on the pixel values of the two datasets—the analysis aimed to quantify the statistical relationship between exposure to TC Irma and urban land use.

Before the regression analysis, both datasets underwent preprocessing to ensure data integrity. The preprocessing involved several steps, including:

**Setting X-limit and Y-limit**

During data preprocessing, a minimum x-limit of 0 and a y-limit of 0.1 were applied. This strategic adjustment excluded pixels representing water from the regression analysis. By implementing these limits, the analysis focused on the relationship between exposure to TC Irma and urban land use.

## 2.4 Future Impact Assessments

This section outlines the methodology for conducting future impact assessments, explicitly focusing on the SSP2 and SSP5 scenarios. The approach centers around harnessing the established relationship derived from the regression analysis to construct exposure projections for the established SSP scenarios. A CC-induced TC Irma based on RCP scenarios was also introduced, utilizing global projections presented by Knutson et al. (2015).

### 2.4.1 Future Urban Land Use Scenarios (SSP's)

Downscaled urban land use projections were available for all the different SSP scenarios. As mentioned, this study explicitly used SSP2 and SSP5 scenarios to construct a time series of projected impacts. SSP2, also called the "middle of the road" scenario, in which the historical trends of economic, social, and technical development remained similar in the future (O'Neill et al., 2017). SSP5 represents a path dominated by extensive fossil-fuel usage, in which rapid development of third-world countries and expedited globalization were considered (O'Neill et al., 2017; Rogelj et al., 2018).

#### 2.4.2 Future Exposure Projections

Future exposure projections were made using the regression formula and the future urban land use projections of SSP2 and SSP5. Firstly, we calculated the difference between the future exposure projections and the "base year" exposure data. This difference was then used to update the future exposure values.

#### 2.4.3 Future Impact Assessment

Future impact analysis was similar to current impact analysis, except it utilizes constructed exposure data frames instead of relying on the exposure data already integrated into CLIMADA. Hereafter, future impact assessments were performed identically to current impact assessments. Firstly, future impact assessments were performed solely using the projections for future urban land use, focusing exclusively on changes in impact caused by changes in urban land. Doing this created a baseline scenario, which can be used as a reference to analyze potential additional impact due to CC (Krichene et al., 2023).

Additionally, future impact assessments were done using future exposure data and projections on TC intensity based on RCPs and the reference year. The intensity of Irma is adjusted based on different RCP scenarios, as introduced Knutson et al. (2015), which show these projections for the RCP4.5 scenarios. By interpolating the RCP values from Knutson et al. (2015) based on their relative radiative forcing, projections for other RCP scenarios were made. The application of RCP scenarios was all done using CLIMADA software. An accurate analysis of the damage ratios could done by implementing CC after first doing an impact analysis based on urban land use change.

### 2.5 Damage Ratio Analysis

This study used SSP/RCP combinations to analyze urbanization-induced and CC-induced damage ratios. Consequently, the composition of future tropical cyclone impact was accurately displayed. Several RCPs can make an SSP scenario "work." Therefore, a damage ratio analysis was done for all possible combinations between SSP2 and SSP5 and the RCPs. Figure 7 displays a table indicating possible RCP and SSP scenarios (Gütschow et al., 2021). SSP2 is compatible with RCP scenarios 1.9, 2.6, 4.5 and 6.0. For SSP5, these are RCP 4.5, 6.0 and 8.5 (Gütschow et al., 2021).

| SSP/RCP | SSP2 | SSP5 |
|---|---|---|
| RCP2.6 | x | - |
| RCP4.5 | x | x |
| RCP6.0 | x | x |
| RCP8.5 | - | x |

Figure 7: Compatible SSP/RCP combinations. 'x' denotes a possible SSP/RCP combination (Gütschow et al., 2021)

Lastly, this study took the projected impact as a percentage of the total US GDP to display the social costs of future TC Irma. The GDP data was provided by the International Institute for Applied System Analysis (IIASA) (Riahi et al., 2017)).

## 2.6 Consistency check relationship urban land use and TC exposure using GDP trends

The comparative analysis between the US GDP and projected TC impact served to assess consistency during the study. This comparison relies on the premise that physical assets, as represented by PC, contribute to GDP. (Wodon and Carey, 2018). The expectation was that the GDP trend and PC impact trends were similar because the amount of direct economic losses due to TCs mainly depends on the proportion of the volume of material assets of a specific region (Schmidt et al., 2009).

# 3 Results

## 3.1 Impact Assessment Results for Base Year Situation

The highest impact was distributed along the tropical cyclone track of Irma, such as Cape Coral, and between Tampa and Orlando. The spatial distribution of impact indicated the model's effectiveness in predicting areas prone to hurricane damage. After running CLIMADA, the model predicted an impact of approximately 72 billion dollars in PC for the base year. Figure 8 indicates where Irma had the most significant impact.

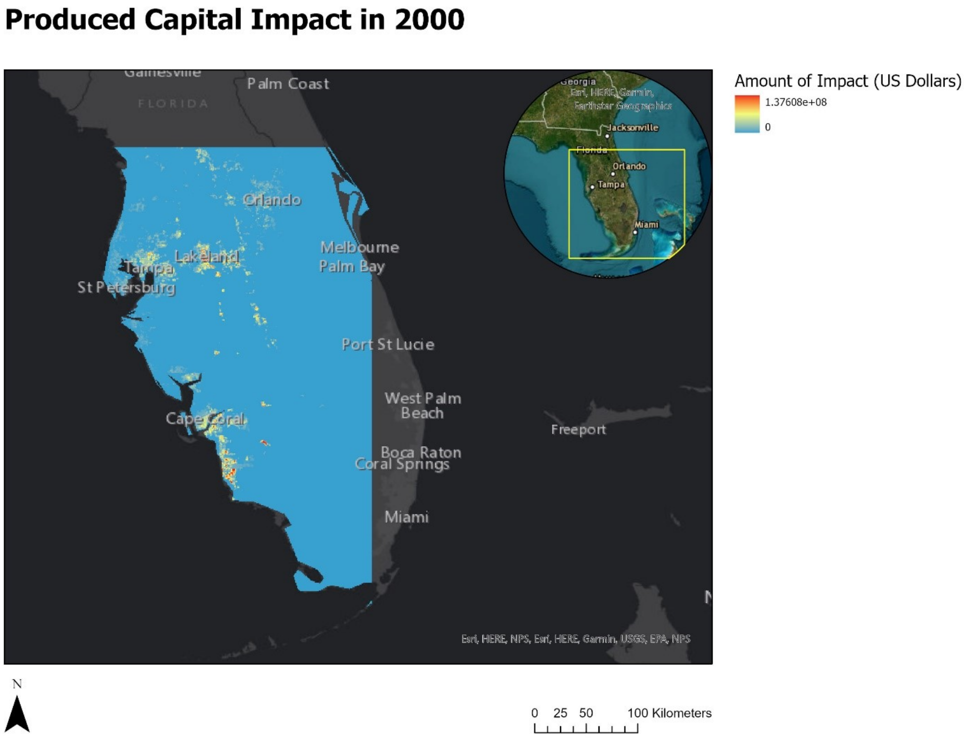


Figure 8: PC impact in 2000

## 3.2 Regression Analysis Results

There is a non-linear relationship between urban land use and TC exposure (Fig. 9). The regression analysis revealed a non-linear trend, as indicated by the curve in the plot. The coefficient of determination (R-squared) was 0.639. This R-squared value indicated that approximately 63.9% of the variability in tropical cyclone exposure can be explained by the non-linear relationship with urban land use (Hagquist and Stenbeck, 1998). The observed non-linear pattern underscored the complex association between urban land use and tropical cyclone exposure because it implies that more variables influence the effect of urban land use on exposure (Ruckstuhl, 2010). New exposure maps were made using the discovered relation and future urban land use maps used in the impact assessments.

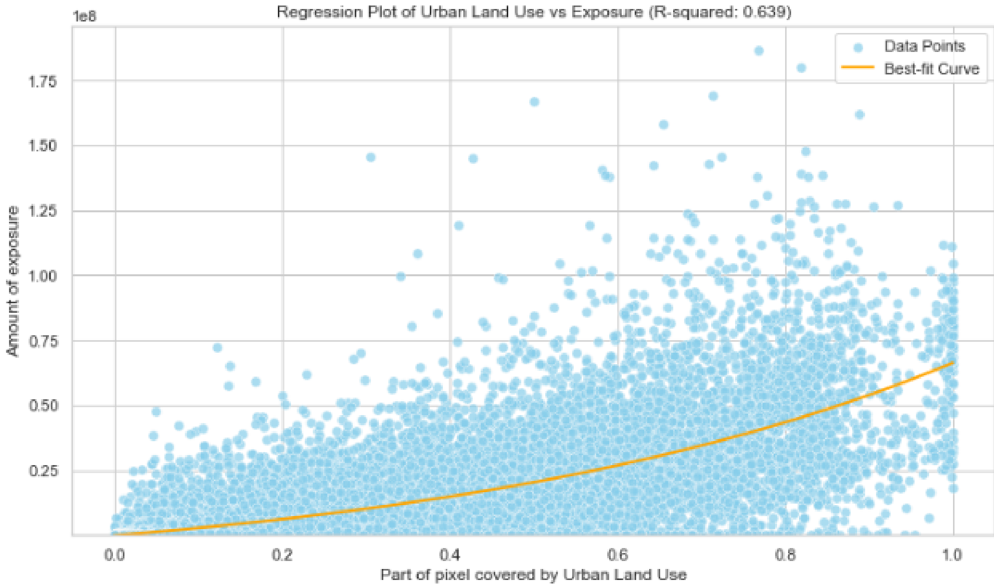


Figure 9: Regression plot of Urban Land Use vs Exposure

### 3.3 Future Exposure and Impact Assessment Results

There was an increase in exposure for every scenario, which followed a similar spatial pattern to urban land use expansion. High exposure rates were found in urban cores and extended outward into rural areas. This progression aligned with the downscaling method outlined in the methods section. It was logical that cells designated for urban land use filled up before developing new areas. Based on the regression analysis, exposure rates should follow the same pattern as urban land use change. Notably, a distinction emerged between the SSP2 and SSP5 scenarios. In the "Middle-of-the-road" SSP2 scenario, urban growth occurred at a comparatively moderate rate, whereas the "fossil-fuel-focused" SSP5 scenario illustrated a substantially accelerated pace of urban expansion.

The spatial patterns in the future impact projections remained similar to those observed in the "base year" (Fig. 10a & Fig. 10b). The highest impact values were concentrated around Cape Coral in the south and between Tampa and Orlando in the north, aligning with the tropical cyclone track of Irma. Notably, there was a significant difference in projected PC impact between SSP2 and SSP5. A notable increase in pixels containing higher impact values indicated an overall rise in impact. With the introduction of a CC-induced hazard, this increase in pixels containing a high value became even more evident (Fig. 10c & Fig. 10d). These maps correspond to combinations of SSP2 with RCP4.5 and SSP5 with RCP8.5

### 3.4 Damage Ratio Analysis

Figures 12 and 11 show a time series plot of urbanization-induced PC impact, CC-induced PC, and the aggregated PC impact for the following SSP and RCP scenario combinations: SSP2 with RCP4.5 and SSP5 with RCP8.5.

The time series under the SSP2 and RCP4.5 (Fig. 12) scenarios revealed dynamic patterns in CC-induced impact, urbanization-induced impact, and the total aggregated impact. The slope of the CC-induced PC impact after 2020 was $9.52 \times 10^8$ US dollars, which was notably smaller than the urbanization-induced PC impact and the aggregated PC impact ($2.40 \times 10^9$ US dollars; $3.36 \times 10^9$ US dollars re-

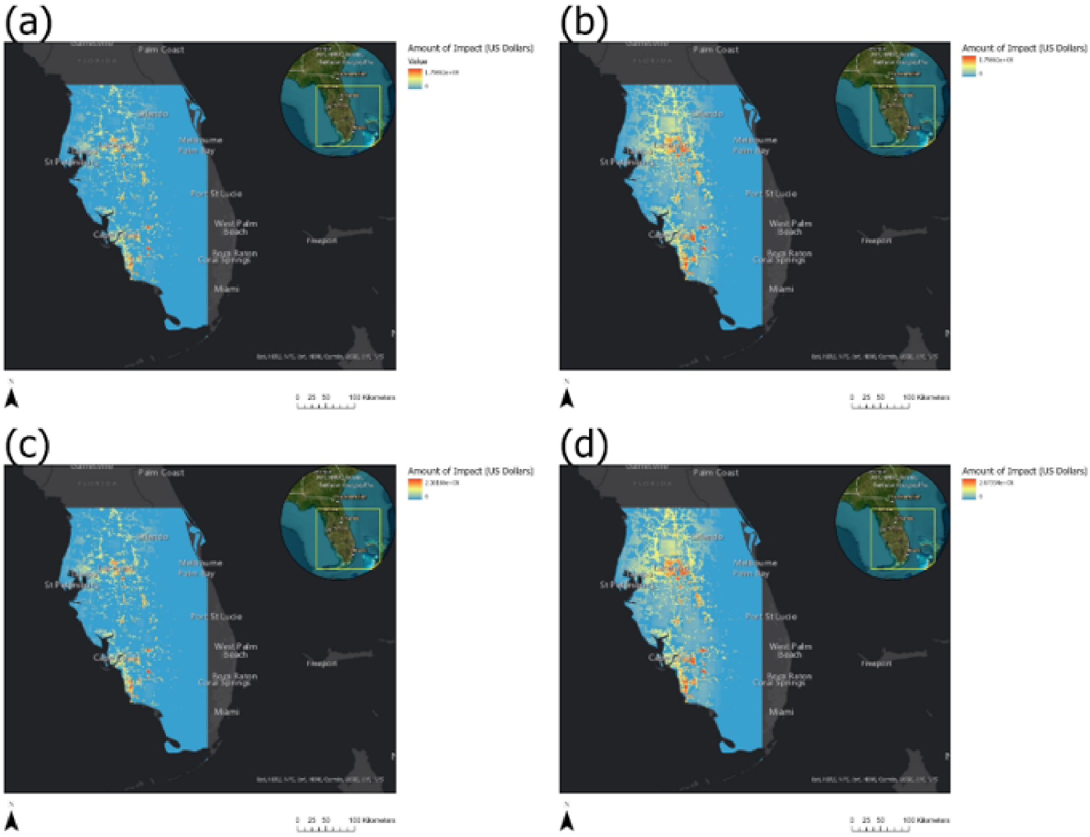


Figure 10: Maps illustrating the projected impacts in 2100 based on urban growth and CC scenarios. Figures (a) and (b) depict impacts solely attributed to urban growth under SSP2 and SSP5, respectively. Figures (c) and (d) demonstrate impacts considering urban growth under SSP2/SSP5 and CC-induced hazards under RCP4.5/RCP8.5, respectively.

spectively). The smaller slope of CC-induced impact indicated a decreasing proportion in the relative contribution of CC to the overall impact.

Conversely, the total aggregated impact exhibited a consistent linear increase, highlighting a cumulative effect over time. The trends suggested that, while the influence of CC may be decreasing in relative terms, the combined impact, driven by both CC and urbanization, is progressively growing.

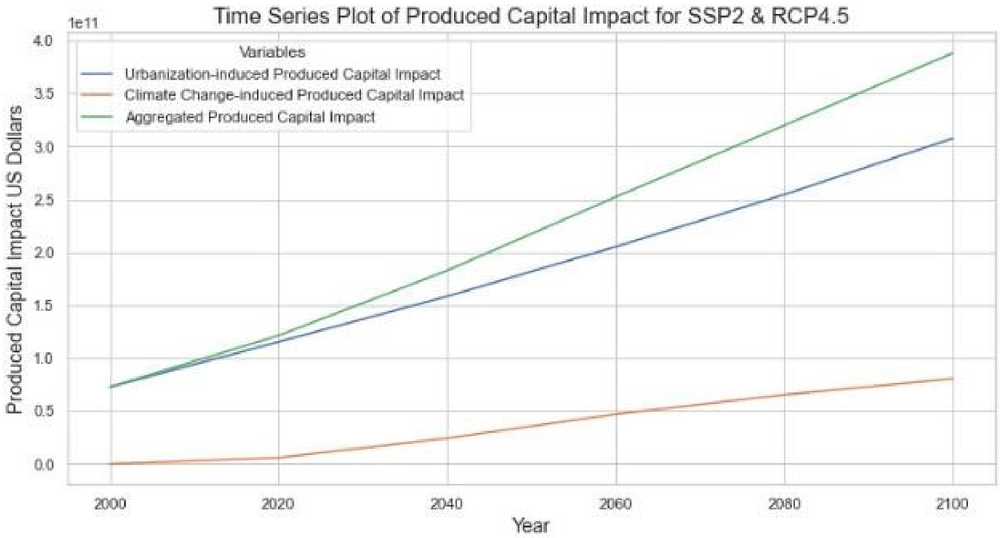


Figure 11: PC Impact of TC Irma under SSP2 & RCP4.5

The time series for the SSP5 & RCP8.5 scenario combination showed a non-linear increase in the PC impact (Fig. 11). The slope of CC-induced impact showed an enlarging trend, increasing from $2.08 \times 10^9$ US dollars between 2020 and 2040 to $1.16 \times 10^{10}$ after 2060. This slope increase suggested a growing relative contribution of CC to the overall impact. Additionally, the share of urbanization-induced damage decreased over time for the SSP5 & RCP8.5 scenario combination. This decrease became apparent because the slope of urbanization-induced changed from $4.5 \times 10^9$ to $8.73 \times 10^9$, which meant that the increase in CC-induced impact was faster than the urbanization-induced impact.

Figure 11 underscored the sensitivity of impact distributions to the severity of CC scenarios. The plots distinctly illustrated that, as the severity of RCP scenarios intensified, the proportion of damage attributed to CC grew accordingly, revealing the distinct influence of CC severity on the overall impact composition.

Figure 13 displays six pie charts representing the impact ratios between CC-induced and urbanization-induced impacts under different SSP and RCP scenarios for the year 2100. A notable trend was evident, highlighting the influence of RCP scenarios on the distribution of impact ratios. The impact ratios indicated a substantial variation between scenarios. In the mildest RCP scenario (RCP2.6) under SSP2, the percentage of the damage attributed to CC was notably low, accounting for only 6.1% of the total impact. In contrast, for the more extreme RCP8.5 scenarios under SSP5, the share of damage induced by CC increased significantly, reaching 45.2%.

Figure 14 demonstrates the importance of adopting a nuanced approach when considering the impact of tropical cyclones (TC). The plot illustrates that the damage as a percentage of GDP decreases for SSP5, characterized by the predominant use of fossil fuels. This decreasing trend likely indicates that economic growth is increasing more quickly than the impact of TC. From the perspective of TC impact, one could perceive this as a more favorable scenario than a milder SSP scenario.

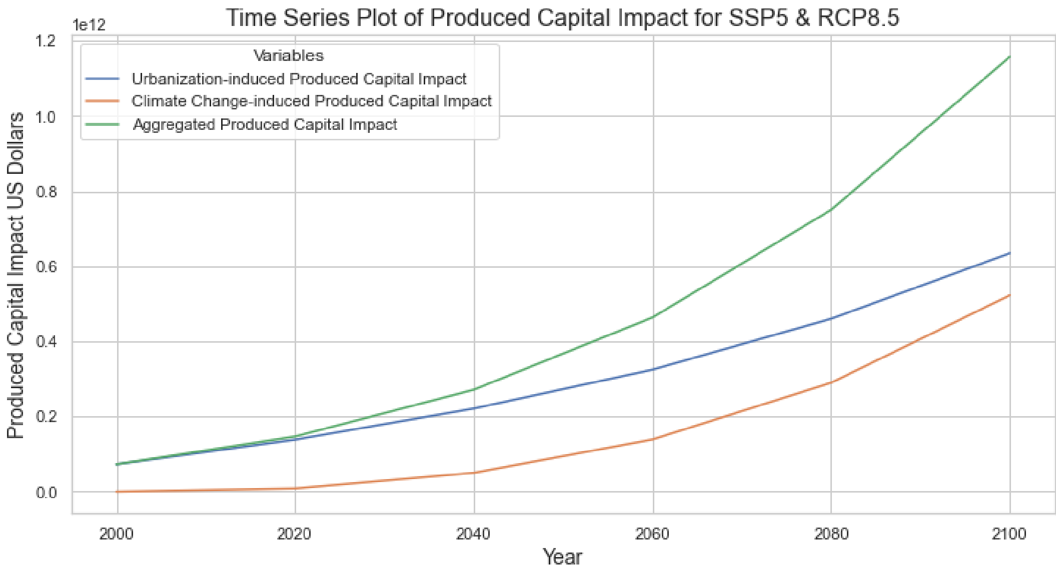


Figure 12: PC Impact of TC Irma under SSP5 & RCP8.5

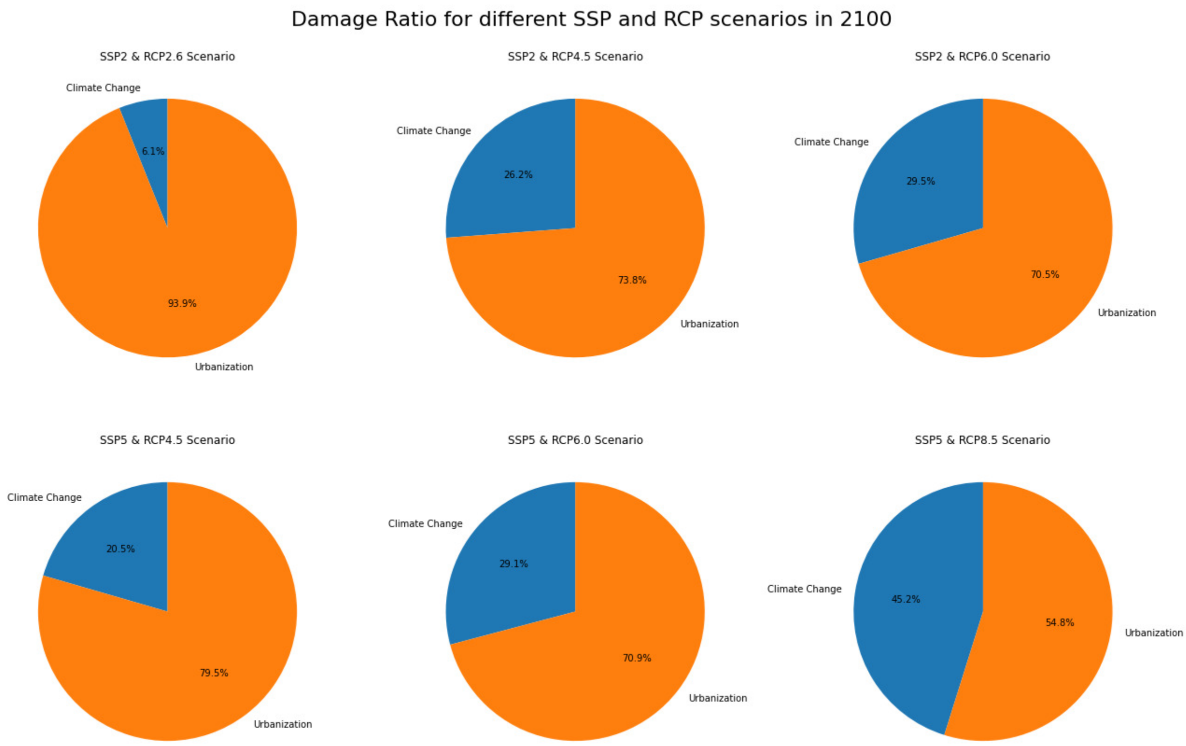


Figure 13: Pie charts for every analyzed SSP/RCP scenario combination in 2100

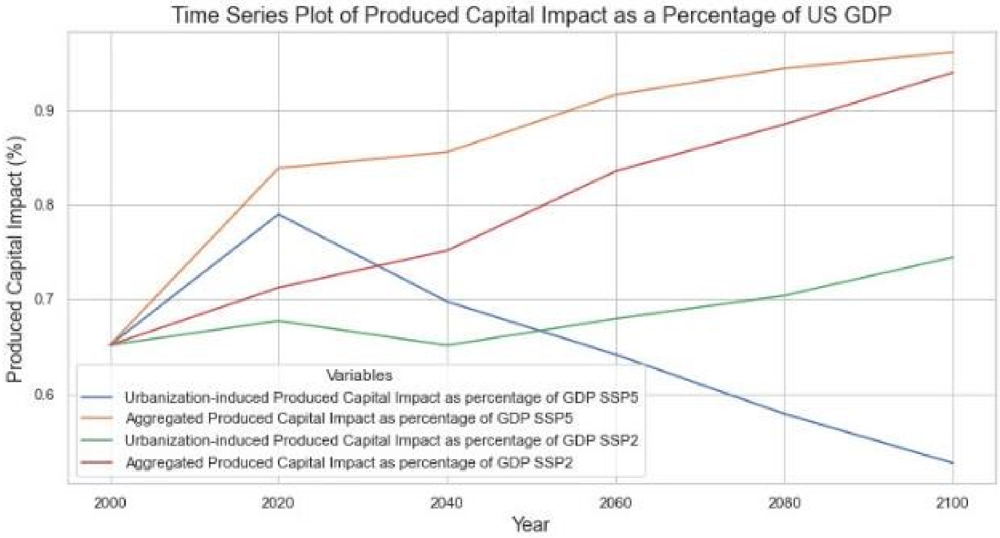


Figure 14: PC Impact as a percentage of US GDP

### 3.5 Consistency Check

The projected increase in PC impact is consistent with the projected US GDP, which serves as a check if these impact projections are reconcilable (Fig. 15 & Fig. 16). This study assessed the coherence of the projected PC impact using a regression analysis between urbanization-induced impact and the projected GDP for the United States under the SSP2 and SSP5 scenarios. The blue area around the trend line represents the 95% confidence interval. The regression plots under both scenarios exhibited a strong linear trend, with an R-squared exceeding 0.99.

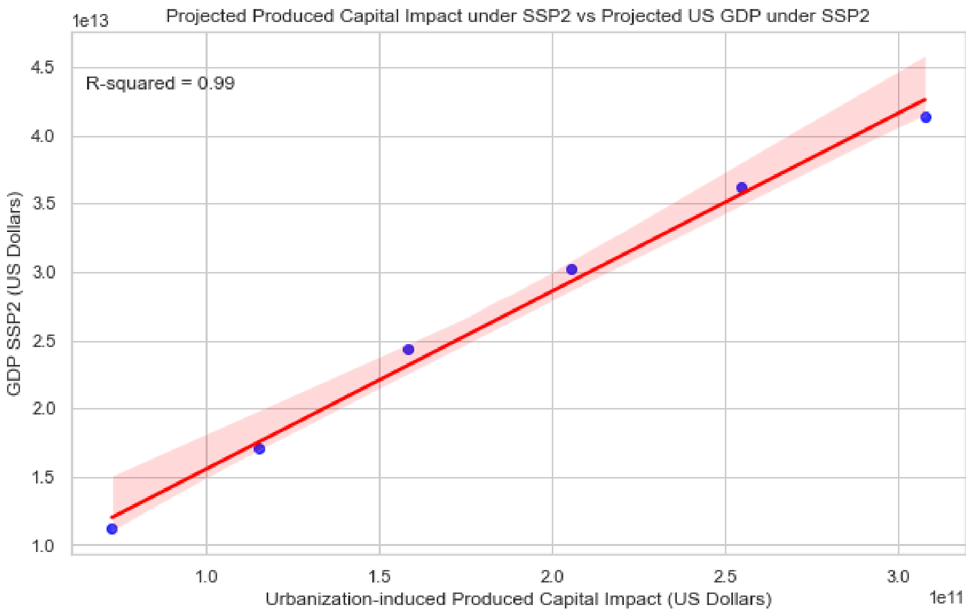


Figure 15: PC Impact under SSP2 vs Projected US GDP

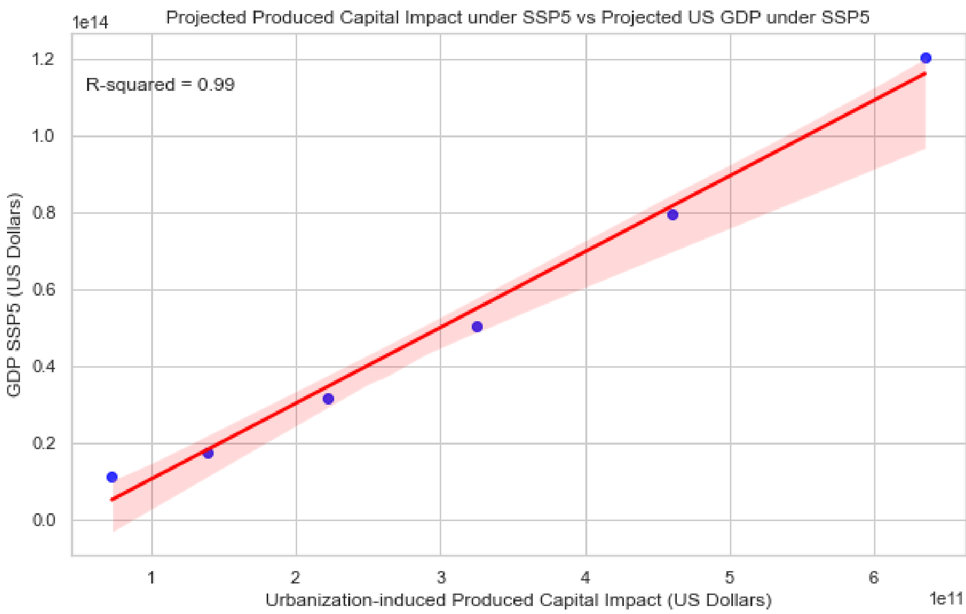


Figure 16: PC Impact under SSP5 vs Projected US GDP

# 4 Discussion

This study found that TC impact increases with urban land use expansion in TC-prone areas, holding hazard and vulnerability factors constant (Strader and Ashley, 2015; Ye et al., 2020). These findings, which suggest that an increase in wealth will lead to an increase in TC impact, agree with those found by (Ye et al., 2020).

Impact assessment of the "base year" situation showed that the model has performed well regarding the spatial distribution of impact. Most of the impact was modeled along the cyclone track of Irma, which was expected when only wind damage was included in the impact assessment.

The damage ratio analysis gave valuable insight into future damage distribution for a future TC Irma. These modeled damage fractions differed remarkably from the damage ratio found by Gettelman et al. (2018). They suggested that for the US, future damage increases are the result of a change in assets and that a change in TCs has no impact. Gettelman et al. (2018) simulated annual mean cyclone damage due to future storms based on historical data, where this study solely focused on Irma in current and future scenarios.

This research applied a consistency check to ensure the reliability of the results. Given that GDP projections based on SSPs were readily accessible and relied on PC (Wodon and Carey, 2018), they were deemed the most suitable assessment tool to ensure the consistency of the study results within the timeframe of this research. Additionally, the anticipated changes in GDP and the impact on PC were likely to align because the direct economic losses from TCs primarily hinge on the proportion of material assets within a given region (Schmidt et al., 2009). Based on this, the future must focus on the spatial planning of urban areas and building regulations for future construction plans (Ye et al., 2020). Furthermore, socioeconomic development and growth require more safety, which gives governments and stakeholders opportunities to invest in prevention or mitigation measures to reduce additional TC risk (Wu et al., 2022). Therefore, economies must act swiftly to foster adaptation within the next decade before the onset of significant CC impacts (Molua et al., 2020). Notwithstanding the above, increasing wealth will eventually lead to higher security demands, necessitating mitigation and protection measures. These measures will ultimately decrease vulnerability (Wu et al., 2018). Higher-income levels reduce TC vulnerability, suggesting socioeconomic development could serve as a crucial method for currently developing nations to enhance their resilience and adaptability concerning CC (Ward and Shively, 2017). Within this framework, more capital becomes invested in vulnerable regions. Consequently, the overall impact on risk becomes uncertain as enhanced protections shift a portion of risk from frequent and low-cost events to rare but high-impact occurrences (Hallegate, 2017). The rise in relative risk exposure also expedites economic advancement. In an optimal developmental trajectory, heightened exposure serves as both a result and a catalyst for economic growth (Hallegate, 2017). A region-specific cost-benefit analysis is an excellent solution to give policymakers and stakeholders better knowledge of potential beneficial mitigation investments and to guarantee the accurate use of those investments (Nguyen et al., 2013). Blanket global policy measures to reduce TC impact may hinder economic progress (Fig. 14) (Hallegate, 2017).

However, return periods of high-impact TCs are likely to decrease due to CC, so caution is needed when considering this approach. (Xu et al., 2020). The SSP/RCP scenario combination, which is compatible with the current trajectories of global development and CC, shows that approximately 25% of the projected impact is a result of CC (Fig. 13). The method used to implement CC in the hazard module of CLIMADA is simplified and solely takes TC frequency and intensity into account. It remains challenging to explain how TC damage will develop in future scenarios since it is still uncertain whether current changes in climate have had a noticeable effect on TCs and whether these changes result from anthropogenic sources (Walsh et al., 2016). It is essential to acknowledge that the modeled impact in the coastal areas may also be lower than the actual impact. This study did not account for surge effects; however, they were substantial in some regions (Pinelli et al., 2018). Additionally, the impact assessment did not incorporate rainfall-induced damages. Rainfall accompanying Hurricane Irma caused inland flooding, power outages, and damage to infrastructure (Bacopoulos, 2019). Consequently, the modeled impact by CLIMADA is lower than the actual impact done by Irma.

Future research should focus on implementing a TC surge and rainfall damage function into the CLIMADA module to account for these limitations. Including these parameters contributes significantly to CC. The CC-induced impact would then include damages attributable to the rising sea levels and the intensification of tropical cyclones (Hoque et al., 2018). Including these factors will lead to an even better damage ratio analysis between socioeconomic and CC-related damages Aznar-Siguan and Bresch (2019).

There are additional elements that contribute to the limitations of this study. Selecting a base year for regression analysis exclusively within that temporal frame may exclude long-term urbanization trends from the analysis. Moreover, the samples employed for regression analysis may exhibit inherent biases (Wang and Cheng, 2020).

The LitPop class used in CLIMADA for exposure assessment overlooks vulnerability and infrastructure specifics, leading to potential inaccuracies (Eberenz et al., 2020). For instance, despite having limited population or nightlight intensity, locations such as mines or power plants carry significant exposure. These discrepancies undermine the regression analysis, reducing its robustness. Incorporating additional local infrastructure data into LitPop datasets can enhance accuracy (Eberenz et al., 2020).

Future urban land use data depends on SSP projections. These projections contain a wide range of uncertainty, which increases successively with each time step (Riahi et al., 2017; Arnell et al., 2019). It is essential to view these SSP scenarios as theoretical projections of development, and they should serve as a foundation for further developing possible future scenarios instead of being seen as realistic scenarios on their own (O'Neill et al., 2014).

Future studies can consider several recommendations. CLIMADA provides a tool to incorporate adaptation measures into the impact assessment. Future research can use this module to incorporate vulnerability into the damage assessment. While preventing TC impact is impossible, proper management strategies can mitigate future damages significantly (Hoque et al., 2018). A cost-benefit calculation can be an appropriate solution to give policymakers and stakeholders better knowledge of potential beneficial mitigation investments. Lastly, additional research should take an enhanced look into the relationship between urban land and exposure. This relationship can be examined more deeply by implementing additional data using stakeholder engagement to explore regions of high exposure but low fractions of urban land. Moreover, Future research should incorporate sensitivity analyses to enhance methodological robustness. Enhancing methodological robustness can involve employing various "base years" and re-conducting regression analyses for each year. Assessing the consistency of regression coefficients across different "base years" can provide valuable insights into potential long-term trends overlooked during initial regression analyses. Additionally, examining whether the regression model maintains consistency across different time steps serves as a reliability test for the model. Using time series regression analysis may benefit future research, encompassing long-term and short-term trends (Imai and Hashizume, 2015).

# 5 Conclusion

The primary aim of this study was to determine how future TC impact is composed and the respective contributions of socioeconomic development and CC. This study has elucidated a non-linear relationship between urban land use and exposure through a regression analysis of Florida's exposure and urban land use data. Integrating socioeconomic variables, such as exposure increase due to urban growth, with projections of a future TC Irma has created a nuanced understanding of how socioeconomic and climate parameters interact and result in TC impact. Future impact assessments under SSP2 and SSP5 scenarios indicated significant increases in TC impact due to urbanization. This study introduced CC by combining the SSPs with the RCPs. Specifically, the pairing of SSP2 with RCP2.6, RCP4.5, and RCP6.0, as well as SSP5 with RCP4.5, RCP6.0, and RCP8.5, including CC into the assessment, revealed an even more significant rise in TC impact.

The performed damage ratio assessments have shown shifting dynamics between CC-induced and urbanization-induced impacts. Urban growth remains the main drive of TC impact; however, under more extreme RCP scenarios, the damage attributable to CC increases significantly. The SSP2/RCP4.5 combination showed a more significant slope of PC impact for urbanization-induced damage ($2.40 \times 10^9$ US Dollars) than for CC-induced PC impact ($9.52 \times 10^8$ US Dollars). This change with a more extreme SSP5/RCP8.5 combination. The CC-induced impact initially increased slower than urbanization-induced damage, with the respective slopes being $2.08 \times 10^9$ US Dollars and $4.15 \times 10^9$ US Dollars. However, this changed at later time steps to a point where after 2060, the slope of CC-induced impact was more significant than the damage caused by urban growth ($1.16 \times 10^{10}$ US Dollars and $8.73 \times 10^9$ US Dollars respectively). The study has shown that the impact ratio of CC-induced impact can vary between 6.1% for the most ideal situation (SSP2/RCP2.6) and 45.2% under the most extreme SSP5/RCP8.5 scenario. These projected PC impact increases were consistent with the projected US GDP, which indicated that the results were applicable.

Based on the results, future mitigation strategies should focus on building regulations and spatial planning. Socioeconomic development urges more significant safety measures, demanding proper investments before the onset of significant CC impact. However, policymaking and mitigation strategy planning should be region-specific, as global blanket strategy planning could hinder economic progress.

The study's limitations include excluding compound events (e.g., TC surge and rainfall), neglect of vulnerability and infrastructure specifics during the impact assessments, and uncertainties within the SSP and RCP projections. Future research should focus on implementing infrastructure specifics and vulnerability with the help of local land use data. Research should implement a cost-benefit analysis to determine appropriate safety measures and mitigation strategies. Lastly, a relationship between urban land and exposure should be further explored by performing regression analyses over multiple timeframes.

In conclusion, this study provided the foundation for continued research into the dynamic relationship between socioeconomic development, CC, and TC impact. Growing TC risk in an increasingly developing and climate-vulnerable world will demand proactive policymaking and integrated approaches to reduce TC impact.

**Data availability**
All scripts and data needed to reproduce the results can be found at https://doi.org/10.5281/zenodo.10664112

# References


Arnell, N. W., Lowe, J. A., Bernie, D., Nicholls, R. J., Brown, S., Challinor, A. J., and Osborn, T. J. (2019). The global and regional impacts of climate change under representative concentration pathway forcings and shared socioeconomic pathway socioeconomic scenarios. *Environmental Research Letters*, 14(8):084046.

Aznar-Siguan, G. and Bresch, D. N. (2019). Climada v1: a global weather and climate risk assessment platform. *Geoscientific Model Development*, 12(7):3085–3097.

Bacopoulos, P. (2019). Extreme low and high waters due to a large and powerful tropical cyclone: Hurricane irma (2017). *Natural Hazards*, 98(3):939–968.

Cameron, A. C. and Windmeijer, F. A. (1997). An r-squared measure of goodness of fit for some common nonlinear regression models. *Journal of econometrics*, 77(2):329–342.

Cardona, O. D., Ordaz, M. G., Mora, M. G., Salgado-Gálvez, M. A., Bernal, G. A., Zuloaga-Romero, D., and González, D. (2014). Global risk assessment: A fully probabilistic seismic and tropical cyclone wind risk assessment. *International journal of disaster risk reduction*, 10:461–476.

Collins, J. M. and Walsh, K. (2017). *TCs and Climate Change*, volume 3. Springer.

Coughlin, K., Bellone, E., Laepple, T., Jewson, S., and Nzerem, K. (2009). A relationship between all atlantic hurricanes and those that make landfall in the usa. *Quarterly Journal of the Royal Meteorological Society: A journal of the atmospheric sciences, applied meteorology and physical oceanography*, 135(639):371–379.

Done, J. M., PaiMazumder, D., Towler, E., and Kishtawal, C. M. (2018). Estimating impacts of north atlantic tropical cyclones using an index of damage potential. *Climatic Change*, 146:561–573.

Eberenz, S., Lüthi, S., and Bresch, D. N. (2021). Regional tropical cyclone impact functions for globally consistent risk assessments. *Natural Hazards and Earth System Sciences*, 21(1):393–415.

Eberenz, S., Stocker, D., Röösli, T., and Bresch, D. N. (2020). Asset exposure data for global physical risk assessment. *Earth System Science Data*, 12(2):817–833.

Emanuel, K. (2011). Global warming effects on us hurricane damage. *Weather, Climate, and Society*, 3(4):261–268.

Freeman, A. C. and Ashley, W. S. (2017). Changes in the us tc disaster landscape: The relationship between risk and exposure. *Natural hazards*, 88(2):659–682.

Gao, J. and O'Neill, B. C. (2020). Mapping global urban land for the 21st century with data-driven simulations and shared socioeconomic pathways. *Nature communications*, 11(1):2302.

Gao, J. and Pesaresi, M. (2021). Global 1-km downscaled urban land extent projection and base year grids by ssp scenarios, 2000–2100. *NASA Socioeconomic Data and Applications Center (SEDAC)*, 3.

Geiger, T., Frieler, K., and Bresch, D. N. (2018). A global historical data set of tropical cyclone exposure (tce-dat). *Earth System Science Data*, 10(1):185–194.

Gettelman, A., Bresch, D. N., Chen, C. C., Truesdale, J. E., and Bacmeister, J. T. (2018). Projections of future tropical cyclone damage with a high-resolution global climate model. *Climatic Change*, 146:575–585.

Gütschow, J., Jeffery, M. L., Günther, A., and Meinshausen, M. (2021). Country-resolved combined emission and socioeconomic pathways based on the representative concentration pathway (rcp) and shared socioeconomic pathway (ssp) scenarios. *Earth System Science Data*, 13(3):1005–1040.

Hagquist, C. and Stenbeck, M. (1998). Goodness of fit in regression analysis–r2 and g2 reconsidered. *Quality and Quantity*, 32(3):229–245.

Hallegate, S. (2017). A normative exploration of the link between development, economic growth, and natural risk. *Economics of Disasters and Climate Change*, 1(1):5–31.

Hoque, M. A. A., Phinn, S., Roelfsema, C., and Childs, I. (2018). Modelling tropical cyclone risks for present and future climate change scenarios using geospatial techniques. *International Journal of Digital Earth*, 11(3):246–263.

Imai, C. and Hashizume, M. (2015). A systematic review of methodology: time series regression analysis for environmental factors and infectious diseases. *Tropical medicine and health*, 43(1):1–9.

Jewson, S. (2021). Conversion of the knutson et al. tropical cyclone climate change projections to risk model baselines. *Journal of Applied Meteorology and Climatology*, 60(11):1517–1530.

Kim, D., Park, D. S. R., Nam, C. C., and Bell, M. M. (2022). The parametric tc rainfall model with moisture and its application to climate change projections. *npj Climate and Atmospheric Science*, 5(1):86.

Knutson, T. R., Sirutis, J. J., Zhao, M., Tuleya, R. E., Bender, M., Vecchi, G. A., and Chavas, D. (2015). Global projections of intense tropical cyclone activity for the late twenty-first century from dynamical downscaling of cmip5/rcp4.5 scenarios. *Journal of Climate*, 28(18):7203–7224.

Korty, R. L., Emanuel, K. A., Huber, M., and Zamora, R. A. (2017). Tropical cyclones downscaled from simulations with very high carbon dioxide levels. *Journal of Climate*, 30(2):649–667.

Krichene, H., Vogt, T., Piontek, F., Geiger, T., Schötz, C., and Otto, C. (2023). The social costs of tropical cyclones. *Nature communications*, 14(1):7294.

Li, Y., Wang, J., Liu, Y., and Long, H. (2014). Problem regions and regional problems of socioeconomic development in china: A perspective from the coordinated development of industrialization, informatization, urbanization and agricultural modernization. *Journal of Geographical Sciences*, 24:1115–1130.

Liang, J. and Liu, D. (2020). Estimating daily inundation probability using remote sensing, riverine flood, and storm surge models: A case of tc harvey. *Remote Sensing*, 12(9):1495.

Meiler, S., Ciullo, A., Kropf, C. M., Emanuel, K., and Bresch, D. N. (2023). Uncertainties and sensitivities in the quantification of future tropical cyclone risk. *Communications Earth & Environment*, 4(1):371.

Mendelsohn, R., Emanuel, K., Chonabayashi, S., and Bakkensen, L. (2012). The impact of climate change on global tropical cyclone damage. *Nature Climate Change*, 2(3):205–209.

Mitsova, D., Esnard, A. M., Sapat, A., and Lai, B. S. (2018). Socioeconomic vulnerability and electric power restoration timelines in florida: the case of hurricane irma. *Natural Hazards*, 94:689–709.

Molua, E. L., Mendelsohn, R. O., and Akamin, A. (2020). Economic vulnerability to tropical storms on the southeastern coast of africa. *Jàmbá: Journal of Disaster Risk Studies*, 12(1):1–14.

Nguyen, T. C., Robinson, J., Kaneko, S., and Komatsu, S. (2013). Estimating the value of economic benefits associated with adaptation to climate change in a developing country: A case study of improvements in tropical cyclone warning services. *Ecological Economics*, 86:117–128.

O'Neill, B. C., Kriegler, E., Ebi, K. L., Kemp-Benedict, E., Riahi, K., Rothman, D. S., and Solecki, W. (2017). The roads ahead: Narratives for shared socioeconomic pathways describing world futures in the 21st century. *Global environmental change*, 42:169–180.

O'Neill, B. C., Kriegler, E., Riahi, K., Ebi, K. L., Hallegatte, S., Carter, T. R., and Van Vuuren, D. P. (2014). A new scenario framework for climate change research: the concept of shared socioeconomic pathways. *Climatic Change*, 122:387–400.

Pinelli, J. P., Roueche, D., Kijewski-Correa, T., Plaz, F., Prevatt, D., Zisis, I., and Moravej, M. (2018). Overview of damage observed in regional construction during the passage of hurricane irma over the state of florida. In *Eighth Congress on Forensic Engineering*, pages 1028–1038, Reston, VA. American Society of Civil Engineers.

Riahi, K., Van Vuuren, D. P., Kriegler, E., Edmonds, J., O'neill, B. C., Fujimori, S., and Tavoni, M. (2017). The shared socioeconomic pathways and their energy, land use, and greenhouse gas emissions implications: An overview. *Global environmental change*, 42:153–168.

Rogelj, J., Popp, A., Calvin, K. V., Luderer, G., Emmerling, J., Gernaat, D., ..., and Tavoni, M. (2018). Scenarios towards limiting global mean temperature increase below 1.5 c. *Nature Climate Change*, 8(4):325–332.

Ruckstuhl, A. (2010). *Introduction to nonlinear regression.* IDP Institut fur Datenanalyse und Prozess-design, Zurcher Hochschule fur Angewandte Wissenschaften.

Schmidt, S., Kemfert, C., and Faust, E. (2009). Simulation of economic losses from tropical cyclones in the years 2015 and 2050: the effects of anthropogenic climate change and growing wealth. 365.

Senkbeil, J. C., Brommer, D. M., and Comstock, I. J. (2011). Tropical cyclone hazards in the usa. *Geography Compass*, 5(8):544–563.

Simpson, N. P., Mach, K. J., Constable, A., Hess, J., Hogarth, R., Howden, M., ..., and Trisos, C. H. (2021). A framework for complex climate change risk assessment. *One Earth*, 4(4):489–501.

Smiley, K. T., Noy, I., Wehner, M. F., Frame, D., Sampson, C. C., and Wing, O. E. (2022). Social inequalities in climate change-attributed impacts of tc harvey. *Nature communications*, 13(1):3418.

Smith, A. B. (2020). 2010–2019: A landmark decade of us. billion-dollar weather and climate disasters. *National Oceanic and Atmospheric Administration.*

Strader, S. M. and Ashley, W. S. (2015). The expanding bull's-eye effect. *Weatherwise*, 68(5):23–29.

Walsh, K. J., McBride, J. L., Klotzbach, P. J., Balachandran, S., Camargo, S. J., Holland, G., and Sugi, M. (2016). Tropical cyclones and climate change. *Wiley Interdisciplinary Reviews: Climate Change*, 7(1):65–89.

Wang, X. and Cheng, Z. (2020). Cross-sectional studies: strengths, weaknesses, and recommendations. *Chest*, 158(1):S65–S71.

Ward, P. J., Blauhut, V., Bloemendaal, N., Daniell, J. E., de Ruiter, M. C., Duncan, M. J., and Winsemius, H. C. (2020). Natural hazard risk assessments at the global scale. *Natural Hazards and Earth System Sciences*, 20(4):1069–1096.

Ward, P. S. and Shively, G. E. (2017). Disaster risk, social vulnerability, and economic development. *Disasters*, 41(2):324–351.

Wodon, Q. and Carey, K. (2018). *The Changing Wealth of Nations 2018*. The World Bank.

Wu, J., Han, G., Zhou, H., and Li, N. (2018). Economic development and declining vulnerability to climate-related disasters in china. *Environmental Research Letters*, 13(3):034013.

Wu, L., Zhao, H., Wang, C., Cao, J., and Liang, J. (2022). Understanding of the effect of climate change on tropical cyclone intensity: a review. *Advances in Atmospheric Sciences*, 39(2):205–221.

Xu, H., Lin, N., Huang, M., and Lou, W. (2020). Design tropical cyclone wind speed when considering climate change. *Journal of Structural Engineering*, 146(5):04020063.

Ye, M., Wu, J., Liu, W., He, X., and Wang, C. (2020). Dependence of tropical cyclone damage on maximum wind speed and socioeconomic factors. *Environmental Research Letters*, 15(9):094061.

Yin, J. (2023). Rapid decadal acceleration of sea level rise along the us east and gulf coasts during 2010–22 and its impact on tc-induced storm surge. *Journal of Climate*, 36(13):4511–4529.